A LABORATORY STUDY OF FRICTION-VELOCITY ESTIMATES FROM SCATTEROMETRY: LOW AND HIGH REGIMES

LARRY F. BLIVEN
NASA/Goddard Space Flight Center
Laboratory for Hydrospheric Processes
Wallops Island, VA 23337, USA

JEAN-PAUL GIOVANANGELI
Institut de Mécanique Statistique de la Turbulence
12 avenue Général Leclerc
13003 Marseille, France

RICHARD H. WANNINKHOF
NOAA/AOML, Ocean Chemistry Dept.
4301 Rickenbacker Causeway
Miami, FL 33149, USA

BERTRAND CHAPRON
IFREMER/Centre de Brest
DRO/OS, BP 70
29270-Plouzane, France

Abstract. Measurements from scatterometers pointing at wind-waves in three large wave-tanks are examined to study fetch effects and the correlation with wind friction-velocity u_*. Time-series measurements were made at 13, 35 and 95 m with a K_a-band scatterometer aimed upwind at 30^o incidence angle and vertical polarization. Average normalized radar cross-section σ_0 values from all fetches follow a common trend for σ_0 as a function of u_*, so the fetch dependence is negligible. An empirical power-law model yields a high correlation between σ_0 and u_*, but because systematic anomalies arise, we reexamine a turbulence approach that delineates low and high regimes with a transition at u_* of approximately 25 cm s^{-1}. Using this criteria, the data are well represented by a two-section power-law relationship between σ_0 and u_*.

The *International Journal of Remote Sensing*
1993. **Vol. 14, No. 9**, 1775-1785.

Homepage: bliven2.osb.wff.nasa.gov
Email: bliven@osb.wff.nasa.gov
Office Phone:757-824-1057

1. Introduction

Satellite based scatterometers offer a practical approach to derive wind vectors over the oceans. The SEASAT satellite mission of 1978 was short lived but analysis of its K_u-band (14.6 GHz) scatterometer data has demonstrated a broad range of potential applications. In addition to oceanic studies, atmospheric investigations benefit from surface wind fields that are used to construct surface pressure maps. Recently ERS-1 was launched and its C-band (5 GHz) scatterometer data will be used for oceanic and atmospheric applications. The air-sea interaction problem is a complex topic with oceanic circulation modeling and wave forecasting being major subjects because of their significant roles in heat flux and gas exchange - which affect weather, climate, and global change.

Momentum fluxes from the wind boundary-layer to the aqueous boundary-layer are quantified in terms of wind friction-velocity u_* at the air-sea interface and these values serve as input for some oceanic circulation models and wave forecasts. Small-scale sea-surface roughness plays an important role in air-sea interaction processes because a major portion of the surface stress is supported by these spectral components. Although *in situ* friction-velocity data are difficult to obtain, *in situ* wind vectors at a reference elevation U_{ref} are more readily available. So drag coefficient models are used to relate wind friction-velocity to the reference wind, ie.,

$$u_*^2 = C_d U_{ref}^2 \tag{1}$$

where C_d is a drag coefficient function. The commonly used SASS-1 model for the SEASAT scatterometer was developed with respect to U_{ref} (Schroeder *et al*. 1982).

Biased friction-velocity estimates cause problems - regardless of the data source. This is illustrated in an oceanic model by Chelton *et al*. (1990), which uses SEASAT scatterometer vector wind observations with directional ambiguities removed by Atlas *et al*. (1987). Generally good results are obtained and the potential for satellite scatterometry to improve and make important contributions to oceanic modeling is described. Yet that basic circulation model also shows that small changes in wind stress estimates result in significant changes in model outcome, so efforts must be made to eliminate or minimize biases.

The SEASAT scatterometer wind retrieval algorithm met system accuracy specifications in an overall sense, however, an error analysis by Woiceshyn *et al*. (1986) reveals systematic biases at low and high winds. Wind speed estimates apparently did not uniformly meet performance criteria. The retrieval algorithm uses a power-law to relate radar cross-section to wind speed and with this formulation, the biases at low and high winds can not be eliminated. Since the biases were observed for all incidence angles, Woiceshyn *et al*. state the necessity for a new model and propose a two segment power-law model.

A two segment model (or wind regimes idea) seems to have been first documented for scatterometer wind-speed algorithms by Duncan *et al*. (1974) (herein DKW), who analyzed data from experiments that were conducted in a wind-wave tank. In that study, a Doppler X-band (9.4 GHz) radar was positioned pointing upwind at 30^o incidence angle and with vertical polarization. At 12 m fetch, the cross section data show (a) greater sensitivity to wind speed changes at low wind speeds than at high wind speeds and (b) that the transition is abrupt at a critical wind speed of about

10 m s^{-1}. Thus a two segment algorithm could be an appropriate relationship between σ_0 and U_{ref}.

Some issues need further investigation. For example, to adequately model all the DKW X-band scatterometer data from 1, 2.75, and 12 m fetches requires different regime model coefficients and transitional wind speeds for each site - so a fetch dependent model is appropriate. Next, there is evidence that σ_0 is more robustly related to u_* than U_{ref} and the necessity of a regimes model between σ_0 and u_* is questionable since Jones and Schroeder (1977) present data from a 13.9 GHz scatterometer (pointing upwind, at 40^o incidence angle) which show a single power-law relationship yields a high correlation without any apparent biases. Unfortunately, friction-velocity was not measured but rather values were derived from U_{ref} measurements using a drag coefficient function. It is well known that there is no definitive drag coefficient function so it is preferable to have boundary layer measurements to derive u_* values.

Thus data are needed of study the relationship between σ_0 and u_* to ascertain (a) fetch effects and (b) the necessity of a regimes formulation. The purpose of this paper is to investigate these issues using data that we obtained in three large wind-wave tanks. Section 2 documents the experimental conditions. Section 3 presents the results with an interpretation based upon boundary-layer observations. Section 4 is a summary with conclusions.

2. Methodology

Scatterometer and wind data for this study are compiled from three laboratory experiments that were conducted to study: the azimuthal variability of a backscattered cross-sections (Giovanangeli *et al*. 1991); the relationship between gas exchange, wind speed and radar backscatter (Wanninkhof and Bliven 1991); and microwave scattering from rain- and wind-roughened seas (Bliven and Giovanangeli 1992). A description of the three wind-wave tank facilities and the scatterometer systems is given in this section.

2.1. *Wind-Wave Tank Facilities*

The *NASA wind-wave tank* is located at Wallops Island, VA, USA. The tank dimensions are 20 m x 1 m x 1.2 m and the operational water depth is 0.7 m. Wind are produced by a suction fan through a closed-loop recirculation system. We filled the tank with fresh water and let the water reach room temperature of about 14 C. The air-water interface was cleaned by a skimming surface-water overnight between experiments and by blowing wind over the water surface before commencing experiments. Wind speed was computed from pitot-tube pressure data obtained at five elevations above the water surface in the center of the tank at 15 m fetch. Profiles of average wind velocity are approximately logarithmic - so a law of the wall model is used to derive u_* values.

The *IMST wind-wave tank* is located in Marseille, France and it is described in detail by Coantic and Farve (1974). The water section is approximately 40 m long, 3 m wide, and 1 m deep. The height of the aerodynamic flow above the water surface is about 1.5 m, and the maximum wind velocity is 14 m s^{-1} (equivalent wind speed at 10 m). The tank was filled with fresh water at a temperature of about 14 C. Wind over the water surface is generated by a large fan in a return duct above the tank. Baffles and screens at each end of the tank make air flow across the entire width of the water channel more uniform. Prior to each run the surface was cleaned by blowing high winds through the tank and lodging surfactants on the downwind beach. Measurements of the longitudinal *u*' and vertical *w*' wind velocity fluctuations were made using a DISA crossed hot-wire sensor connected to two DISA model 55 constant-temperature anemometers. The cross-wire sensor is calibrated in a small wind tunnel and due to the high intensity of velocity fluctuations close to the water-waves, the nonlinear cooling law of Giovanangeli (1980) is used to derive u' and w'. Friction-velocities were computed using the relationship $u_* = \langle -u'w' \rangle^{1/2}$, where <> means time average. Results reported by Giovanangeli *et al*. (1991) show that there is a constant flux shear-layer above the air-water interface.

The *Delft Hydraulics (DH) wind-wave tank* is located in Delft, the Netherlands. This is a "T" shaped wind-wave tank. The main channel water section was effectively 100 m long and 8 m wide because although the last 9 m of the tank is 25 m wide, the side lobes were isolated by a plexiglass wall. We were interested in obtaining data at very high wind speeds, so a water depth of 70 cm (instead of the normal 80 cm) was used in order to prevent waves from spilling into the return air-duct. The air space is 10 m wide and 2 m high expect for the last 9 m, which is approximately 10 m high. The tank contained fresh water with a temperature of ~14 C. Wind over the water surface is generated by a large fan in a return duct underneath the tank, which has baffles and screens located at each end. Wind speeds of up to 21 m s^{-1} (equivalent wind speed at 10 m height) can be attained with the fan. Prior to each run the surface was cleaned by blowing a 2.5 m s^{-1} wind over the tank and skimming the surfactants off the surface with a trough at the downwind end. We measured reference wind speeds with two anemometers at 88 m downwind from the tunnel inlet. The anemometers were suspended 80 cm below the ceiling and 2 m from the side. During 1988, the Royal Dutch Meteorological Institue (KNMI) conducted wind-profile measurements as part of the Dutch-German VIERS project and an empirical relationship was developed between the reference wind speed and friction-velocity.

2.2. Scatterometer

A K_a-band radar system was the primary scatterometer used for this study. A schematic of this 36 GHz (8 mm wavelength) system has been presented by Bliven and Norcross (1988) and examples of cross-section time series data were presented by Bliven *et al*. (1988). We used a standard procedure (Schroeder *et al*. 1984) to calibrate the radar. Data are normalized relative to the return from a 15 cm diameter metal sphere at a range equal to the centerline distance to the calm water surface. For each wind speed, we digitized the analog return signals from the scatterometer and computed average voltages. Normalized radar cross-section σ_0 is computed as the ratio of the average voltage to that of a 15 cm diameter metal sphere at the appropriate range. These values are converted to decibel units (dB) according to the formula

$$\sigma_0(dB) = 10 \log \sigma_0 \quad . \qquad \textbf{(2)}$$

The scatterometer has operated in the wind-wave tanks at 1 m or 1.5 m range to the calm water surface. The alignment was at 30^o inclination from nadir and vertical polarization was used for both transmit and receive horns. With this setup, the radar footprint diameter at 1 m range to a calm water surface is approximately elliptical with dimensions of 12 x 10 cm^2.

We conducted several validation tests. For wind roughened surfaces in a wind-wave tank, we found that there is negligible backscattered power at frequencies above about 25 Hz. The standard error of σ_0 estimates decreases inversely with $time^{1/2}$ and a 20 minute data set yields a standard error of about 3.5 percent. To ensure that measurements within each wind-wave tank are not contaminated by reflections from unwanted secondary targets beyond the water surface, we conducted azimuthal response tests. With the scatterometer pointing at the calm water surface, we rotate the radar to vary the azimuthal angle and we watch for variations in the output. If there is an object with a shape like a corner reflector, then the signal level is enhanced. So objects that act like corner reflectors in the field of view are removed and the response is essentially isotropic. Thus the system has a reproducible calibration so data from different facilities and setups is compared without preprocessing or adjustments.

3. RESULTS AND ANALYSIS

3.1. Fetch Effects

K_a-band cross-section measurements at 13.5, 35 and 95 m are shown as a function of friction-velocity in figure 1. The measurements are rather distinctive because: the u_* values span a wide range so that conditions vary from very light winds to extremely high winds; the data density is quite high so that fine structure of the σ_0 dependence can be closely examined; and the data are from three different fetches. In all cases, the scatterometer was pointing upwind at an incidence angle of 30^o and both transmit and receive antennae were set for vertical polarization. The analog radar backscattered power were digitized as follows: 100 Hz for a total of 128 K data points at NASA; 100 Hz for a total of 32 K data points at IMST; and 80 Hz for a total of 20 K data at DH. The standard error of the mean values is less than ~0.7 dB, which is approximately the size of the symbols in figure 1. As previously stated, wind friction-velocities were estimated from pitot tube measurements of the wind profile at NASA, from hot-wire anemometer data at IMST, and from cup anemometer measurements at Delft. Figure 1 shows that all the σ_0 data conform to a single trend with respect to u_*. The negligible fetch dependence implies that friction-velocity is the principal parameter for determining σ_0 when small-scale roughness is the dominant mechanism for momentum flux.

Another laboratory investigation was conducted by Duncan *et al*. (1974), who reported on the fetch and wind speed dependence of cross-sections at short fetches in wave-tanks. In particular, measurements were made with an X-band scatterometer pointing upwind with vv polarization and 30^o incidence angle at 1, 2.75 and 12 m fetches. The results are presented in terms of σ_0 and U_{ref}. At light wind speeds, some cross-section values differ by up to 20 dB for similar wind speeds. At high winds, the values from 1 m fetch are about 3 dB less than from the other sites. At 12 m fetch, the transition between the high sensitivity at low winds and lower sensitivity (approximately linear) at high winds occurs at a winds speed of about 10 m s^{-1}, which Duncan *et al*. associate with the wind speed where vigorous wave breaking begins to occur. Because the data from 1 and 2.75 m are vastly different compared to the data from 12 m, it is difficult to interpret the σ_0 data simply in terms of U_{ref} and it is tenuous to draw general conclusions from the observations obtained at any one site.

Further experiments and analysis are needed to model microwave scattering from wind-roughened water surfaces at exceedingly short fetch, where wind-generated drift-currents in the water surface-layers are uncommonly high, inhomogeneous, and turbulent. At longer fetches, the K_a-band scatterometer measurements show a consistent trend for σ_0 with respect to u_*, so we proceed with an appraisal of fetch-independent empirical models.

3.2. Global Power-Law Model

Model. A power-law relationship between σ_0 and U_{ref} was suggested by Guinard *et al*. (1971) and Bradley (1971) and since then it has been routinely used to define a relationship between scatterometer cross-section and wind speed as

$$\sigma_0 = G(\theta,\phi,pol)\,U_{ref}^{H(\theta,\phi,pol)} \qquad \textbf{(3)}$$

where θ is the azimuthal direction (0 for the radar pointing upwind) and ϕ is the incidence angle measured from nadir. We refer to this as a 'global' power-law model because G and H are not a function of wind-speed.

The global power-law model for wind scatterometry was revised by Jones and Schroeder (1977), who investigated the dependence of radar backscatter on surface friction-velocity using an empirical power-law relationship given by

$$\sigma_0 = G^*(\theta,\phi,pol)\,u_*^{H^*(\theta,\phi,pol)} \qquad \textbf{(4)}$$

This is a global power-law model for friction-velocity scatterometry. An alternate form of Equation 4 is used when radar data are presented in logarithmic format, i.e.

$$\sigma_0(dB) = G^*(dB) + H^*(10\log u_*) \quad . \qquad \textbf{(5)}$$

Application. The 36 GHz data are compared to a global power-law relationship for friction-velocity scatterometry in figure 1. The coefficients G^*(dB) and H^*, derived by a least-squares technique, are -33.22 dB and 1.77 dB s cm^{-1} respectively. The correlation coefficient R^2 is 0.97, which indicates good overall agreement between the model and the data.

There appears to be systematic deviations between the model and these data, so we computed normalized residual values as

$$\delta = \frac{\sigma_0(model) - \sigma_0(measured)}{\sigma_0(measured)} \quad . \qquad \textbf{(6)}$$

The residuals are shown as a function of friction-velocity in figure 2, in which bias patterns clearly emerge. These biases are impossible to eliminate using a global power-law relationship, so alternative formulations need consideration.

3.3. *Regimes Power-Law Model*

Model. A simple modification of the global power-law relationship is a two section model that represents different ranges of friction-velocity. We postulate that the change is related to air-sea interaction processes that effect the short wavelength spectral region. Since the data suggest a well defined transition from a low to high regime, physical models that define a transition criteria seem appropriate. Consequently, we will review a boundary-layer representation that offers a heuristic physical basis for a transition between low and high regimes for small-scale air-sea interaction processes.

Boundary-layer physics is the basis for several papers by Wu (1969a, 1969b, 1980, 1986), who investigated momentum fluxes in the air-sea boundary-layer by measurements that were used to characterize *bulk parameters* such as the roughness length-scale. The roughness length-scale data show a transition at a friction-velocity of 26.3 cm s^{-1}. Because this is close to the minimum phase-speed for capillary-gravity waves, Wu proposed that airflow over a wind-disturbed water surface separates from short-waves with phase velocities smaller than the wind friction-velocity.

Similar conclusions were derived from analysis of boundary-layer data in the *time domain*. Flow visualization and other techniques show an association between air-flow separation and wave breaking (Banner and Melville 1976, Gent and Taylor 1977). Melville (1977) uses that finding to define a transition from aerodynamically smooth to rough flow, which he relates to the onset of extensive small-scale wave breaking. He proposes that since small-scale wave breaking is associated with generation of turbulence in the wind boundary-layer, the transitional friction-velocity is approximately equal to the phase velocity of breaking waves - even when the small waves are riding on swell. Melville concludes that due to the existence of a minimum phase velocity for surface waves, there is a minimum friction-velocity (about 23 cm s^{-1}) below which rough flow cannot occur.

Wave dissipation and probably wave generation are different in the low and high regimes. These processes are not presently fully understood so the functional dependence of wavenumber spectra on u_* can not be derived analytically with complete certainty. Consequently the functional dependence between σ_0 and u_* is also ambiguous. The boundary-layer measurements and models suggest, however, that the low and high regimes are significantly different so it is reasonable to study the relationship between σ_0 and u_* separately within each regime.

Application. If we assume that the transition between high and low regimes for scatterometry is related to boundary-layer processes, then the transitional u_* is in the range of 23 to 26 cm s^{-1}. We will use 25 cm s^{-1}. Additionally, an empirical model for each regime needs to be specified so we assume a power-law relationship between σ_0 and u_* for each regime. This approach permits the findings to be easily compared to previous results.

The 36 GHz data are compared to the regimes model in figure 3, which shows that the data are well dispersed around the empirical model and that the power-laws vary considerably between regimes. Indeed the G^* and H^* coefficients derived by a least-squares technique are -39.46 dB and 2.36 dB s cm^{-1} for the low regime and -18.96 dB and 0.93 dB s cm^{-1} for the high regime. The residuals between measurements and model are shown as a function of friction-velocity in figure 4, which shows that the data are distributed around the abscissa with no particular pattern.

We also made measurements with a K_u-band scatterometer at DH at the 95 m fetch. This 13.5 GHz system was pointed upwind at an incidence angle of 30^o and both transmit and receive antennae were set for vertical polarization. The analog radar backscattered power was digitized at 80 Hz for a total of 20 K data and then processed using the same procedures as for the K_a-band system. Figure 5 shows that the K_u-band data are also well modeled by the boundary-layer regimes model. Again the power-laws vary considerably between regimes with G^* and H^* coefficients in the low and high regimes of (-32.32 dB, 1.76 dB s cm^{-1}) and (-19.54 dB, 0.92 dB s cm^{-1}).

The regimes approach is useful for modeling these laboratory K_u- and K_a-band scatterometer data. The results show that the power-law exponent is much greater for the low regime than for the high regime. In the high regime, σ_0 is approximately a linear function of u_*. Although the high regime sensitivity is considerably less than that of the low regime, the data do not saturate. To delineate regimes, the model uses u_* of 25 cm s^{-1} as the critical friction velocity. For steady winds blowing over clean water surfaces in wind-wave tanks, the regimes are rather well defined for σ_0 as a function of u_*. For field conditions, natural fluctuations of the wind can be expected to act as a smoothing function - so the transition is probably less distinct. *In situ* validation is necessary for all algorithms and due to the uncertainty in drag coefficient models, it is prudent to actually measure u_* to ascertain the need for a regimes scatterometer u_* model.

4. CONCLUSIONS

We have examined microwave scattering from wind-waves in three large wave-tanks using radar and wind data obtained at 13, 35 and 95 m. A K_a-band scatterometer was pointed upwind at 30^o incidence angle and with vertical polarization. Friction-velocities were estimated from air boundary-layer measurements of either turbulent wind components or mean velocity profiles and the u_* values span from 5 to 100 cm s^{-1}, which represents light wind to whole gale. For all three fetches, a consistent pattern of σ_0 as a function of u_* is found and although a power-law model yields good overall agreement, systematic biases appear - so a global power-law relationship may be inadequate for a scatterometer friction-velocity algorithm. A transition from high sensitivity at lower friction-velocities to lower sensitivity at higher friction-velocities occurs at about 25 cm s^{-1}. This is approximately the critical friction-velocity of a turbulence model that delineates regimes by the onset of wind boundary-layer flow-separation and wave-breaking. The laboratory data are well modeled by a two segment power-law model with a transition at 25 cm s^{-1}, so we recommend that *in situ* studies investigate models that can simulate this feature.

The use of friction velocity, rather than a reference wind speed, may also facilitate modeling of boundary-layer stability effects (Li *et al*. 1989) and azimuthal variability (Giovanangeli *et al*. 1991), so u_* seems to be a robust parameter for determining σ_0. A simple scaling law between σ_0 and u_* is perhaps viable, thus development and calibration of scatterometer wind retrieval algorithms should place a high priority on acquiring u_* data.

Acknowledgments. We are grateful to our colleagues who participated in this research and in particular, B. Zucchini, A. Laurence, and R. Vaudo provided indispensable technical support. We thank KNMI, who provided windspeed measurements and friction-velocity calculations for the DH study component as part of the Dutch/German 'VIERS' project. NASA (RTOP 972-161-80-28), the Office of Naval Research (ONR 972-146-70-11), the Centre National de la Recherche Scientifique, the Direction des Recherches, Etudes et Techniques, the PAMOS committee, and National Science Foundation grant OCE 87-11184 contributed funding for this research.

References

ATLAS, R., BUSALACCHI, A.J., GHIL, M., BLOOM, S., and KALNAY, E., 1987, Global surface winds and flux fields from model assimilation of Seasat data. *Journal Geophysical Research*, **92**, 6477-6487.

BANNER, M.L. and MELVILLE, W.K., 1976, On the Separation of Air Flow Over Water Waves. *Journal of Fluid Mechanics*, **77**(4), 825-842.

BLIVEN, L.F., GIOVANANGELI, J-P, and NORCROSS, G., 1988, A study of rain effects on radar scattering from water waves. *Proceedings of the 7th Conference on Ocean-Atmosphere Interactions of American Meteorological Society* held in Anaheim, California, on 1-5 February 1988, Boston, MA: American Meteorological Society D(VT) 500 1/88, 230-233.

BLIVEN, L.F. and NORCROSS, G., 1988, Effects of rainfall on scatterometer derived wind-speeds. *Proceedings of the IGARSS'88* held in Edinburgh, Scotland, on 12-16 September 1988, ESA SP-284 (Paris: European Space Agency), **1**, 565-566.

BLIVEN, L.F. and GIOVANANGELI, J-P, 1992, An experimental study of microwave scattering from rain- and wind-roughened seas, *International Journal of Remote Sensing*, in press.

BRADLEY, G.A., 1971, *Remote sensing of ocean winds using a radar scatterometer*, (Lawrence, KA: University of Kansas).

CHELTON, D.B., MESTAS-NUNEZ, A.M., and FREILICH, M.H., 1990, Global wind stress and Sverdrup circulation from the Seasat scatterometer, *Journal Physical Oceanography*, **20**, 1176-1205.

COANTIC, M. and FAVRE, A., 1974, Activities in and preliminary results of air- sea interaction research at IMST. *Advances in Geophysics*, **16**, 391-405.

DUNCAN, J.R., KELLER, W.C. and WRIGHT, J.W., 1974, Fetch and Wind Speed Dependence of Doppler Spectra. *Radio Science*, **9**(10), 809-819.

GENT, P.R., AND TAYLOR, P.A., 1977, A note on 'separation' over short wind waves, *Boundary Layer Meteorology*, **11**, 201-213.

GIOVANANGELI, J-P., 1980, A nondimensional heat transfer law for a slanted hot film in water flow, *DISA Information*, 12.

GIOVANANGELI, J-P., BLIVEN, L.F., and LE CALVE, O., 1991, A wind-wave tank study of the azimuthal response of a Ka-band scatterometer. *I.E.E.E. Journal Geoscience and Remote Sensing*, **29**(1), 143-148.

GUINARD, N.W., RANSONE, J.T., JR., and DALEY, J.C., 1971, Variation of the NRCS of the sea with increasing roughness, *Journal Geophysical Research*, **76**, 1525-1533.

JONES, L.W. and SCHROEDER, L.C., 1977, Radar Backscatter From the Ocean Dependence on Surface Friction Velocity. *Boundary-Layer Meteorology*, **13**, 133-149.

LI, F., LARGE, W., SHAW W., WALSH, E.J. and DAVIDSON, K., 1989, Ocean radar backscatter relationship with near-surface winds: a case study during FASINEX. *Journal of Physical Oceanography*, **19**, 342-353.

MELVILLE, W.K., 1977, Wind Stress and Roughness Length Over Breaking Waves. *Journal of Physical Oceanography*, **7**, 702-710.

SCHROEDER, L.C., BOGGS, D.H., DORNE, G., HALBERSTRAM, I.M., JONES, L.W., PIERSON, W.J. and WENTZ, F.J., 1982, The relationship between wind vector and normalized radar cross section used to derive Seasat A satellite scatterometer winds. *Journal Geophysical Research*, **87**(C5), 3318-3336.

SCHROEDER, L.C., JONES, W.L., SCHAFFNER, P.R., AND MITCHELL, J.L., 1984, Flight measurement and analysis of AAFE RADSCAT wind speed signature of the ocean, *(Washington, D.C.: NASA Technical Memorandum 85646)*.

WANNINKHOF, R.H. and BLIVEN, L.F., 1991, Relationship between gas exchange, wind speed, and radar backscatter in a large wind-wave tank, *Journal of Geophysical Research*, **96**(C2), 2785-2796.

WOICESHYN, P. M., WURTELE, M.G., BOGGS, D.H., MCGOLDRICK, L.F. and PEREHERYCH, S., 1986, The Necessity for a New parameterization of an Empirical Model for Wind/Ocean Scatterometry. *Journal of Geophysical Research*, **91**(C2), 2273-2288.

WU, J., 1969a, Wind stress and surface roughness at air-sea interface. *Journal Geophysical Research*, **74**(2), 444-454.

WU, J., 1969b, A criterion for determining air-flow separation from wind waves. *Tellus*, **21**, 707-713.

WU, J., 1980, Wind Stress Coefficients Over Sea Surface Near Neutral Conditions-A Revisit, *Journal of Physical Oceanography*, **10**(5), 727-740.

WU, J., 1986, Roughness Elements of the Sea Surface-Their Spectral Composition. *Tellus*, **38A**, 178-188.

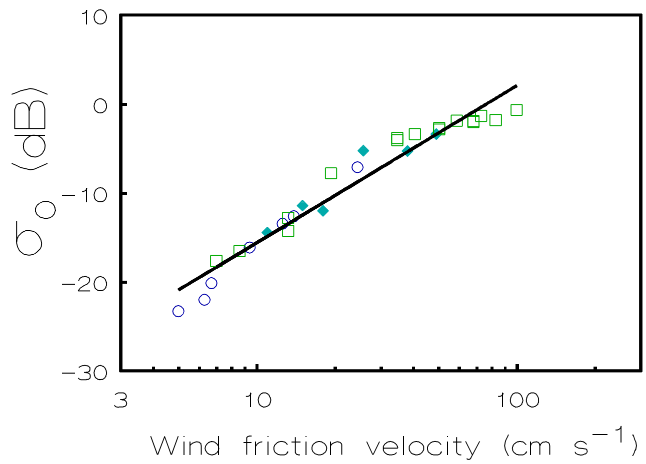

Figure 1. K_a-band scatterometer (upwind, 30^{o} incidence angle, v pol) σ_0 values from 13.5, 35 and 95 m fetches (○, ♦, □). The data follow a consistent trend as a function of u_* with negligible fetch dependence. An empirical power-law model is compared to the K_a-band data and it provides a good overall representation.

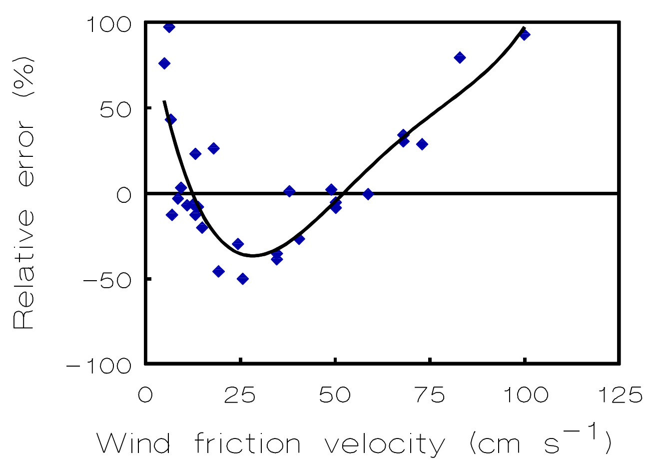

Figure 2. Normalized residuals between power-law model estimates and the K_a-band observations show a pattern as a function of u_*, so alternative models need to be considered.

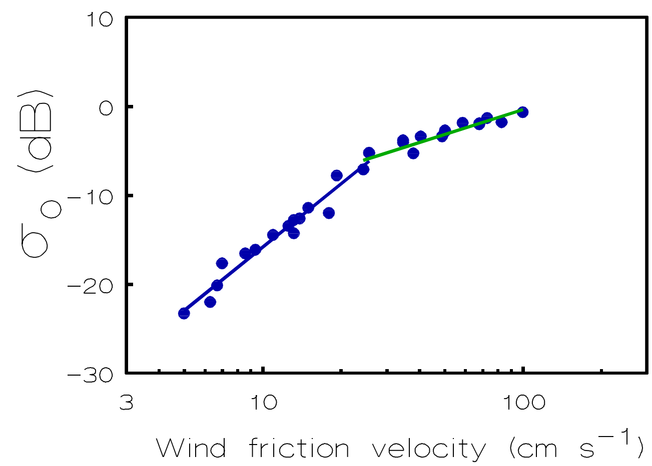

Figure 3. A regimes model with a transition at $u_* = 25$ cm s^{-1} fits the K_a-band data well. The power-law exponents for the low and high regimes are considerably different, being 2.36 and 0.93 dB s cm^{-1} respectively, so the regimes are quite dissimilar.

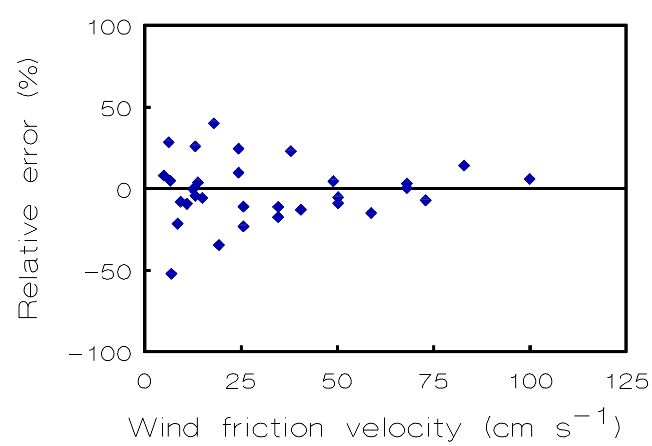

Figure 4. Normalized residuals between the regimes model and the K_a-band data show no distinctive pattern as a function of u_*. So the regimes model predictions are well behaved.

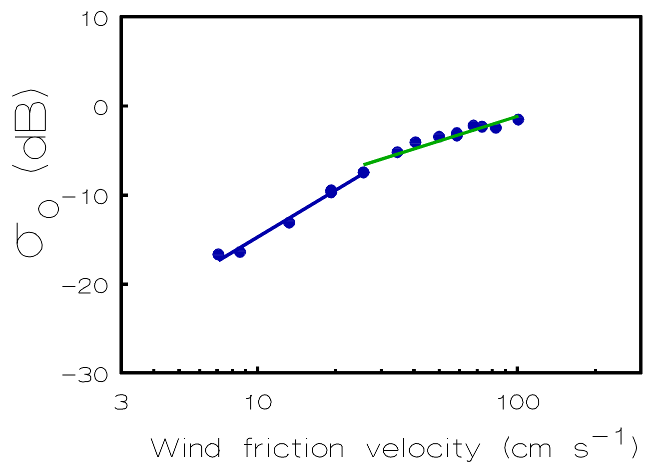

Figure 5. The regimes model (transition at $u_* = 25$ cm s^{-1}) shows good agreement with K_u-band scatterometer data (upwind, 30^o incidence angle, v pol) from 95 m fetch. The power-law exponents for the low and high regimes are 1.76 and 0.92 dB s cm^{-1}.